ChemComm

COMMUNICATION

View Article Online
View Journal | View Issue

Cite this: *Chem. Commun.*, 2023, 59, 11113

Received 29th June 2023,
Accepted 21st August 2023

DOI: 10.1039/d3cc03145d

rsc.li/chemcomm

Solvent-free room-temperature synthesis of brightly luminescent $[BMPyr]_2[SnCl_4]$†‡

Silke Wolf and Claus Feldmann *

The pseudo-ternary tin(II) halide $[BMPyr]_2[SnCl_4]$ can be obtained just by mixing the starting materials [BMPyr]Cl and $SnCl_2$ at room temperature without additional solvents. The compound shows bright Sn(II)-based emission of deep-red light (λ_{max}: 740 nm) with a quantum yield of 88 ± 3% after optimised synthesis. Characterization is performed by X-ray structure analysis, infrared and fluorescence spectroscopy. Exemplary fluorescent thinfilms are realized by solvent processing.

Chemical syntheses with ionic solids as starting materials and/or products are usually performed either in solution or *via* solid-state reactions.[1] To this regard, the diffusion of ions either requires a dissolution of the ionic solid with formation of solvato complexes or an increased Brownian motion in the solid state at elevated temperature. Two recent developments allow to expand the toolbox for chemical syntheses significantly. On the one hand, ionic liquids as polar and weakly coordinating solvents offer the option for reactions near room temperature (≤100 °C) without the necessity to form solvato complexes for the dissolution of the starting materials.[1,2] Here, the realization of a range of spectacular compounds already impressively illustrated the benefit of ionic liquids for chemical synthesis.[3] On the other hand, organo-metal halides with large organic cations and inorganic complex anions turned out to be well-soluble in organic solvents such as DMSO or DMF.[4] Here, methylammonium lead iodide ($[CH_3NH_3]PbI_3$) is a most prominent example,[5] which – in addition to the advantage of its high efficiency as a solar absorber – can be processed in solution (*e.g.*, DMF, DMSO).[4] Beside solid-state reactions and solution-based synthesis, a room-temperature synthesis of ionic solids in absence of additional solvents is rare.

For $[BMPyr]_2[SnCl_4]$ (BMPyr: 1-butyl-1-methylpyrrolidinium), we observed that the synthesis can be performed already at room temperature, simply by mixing the starting materials [BMPyr]Cl and $SnCl_2$. The course of the reaction can be followed by the naked eye based on the red emission of $[BMPyr]_2[SnCl_4]$, whose intensity correlates with its proceeding formation. $[BMPyr]_2[SnCl_4]$ shows an unusual disphenoidal $[SnCl_4]^{2-}$ anion and, after optimized reaction, intense deep-red Sn^{2+}-based emission with an unexpected high quantum yield of 88 ± 3%.

The synthesis of $[BMPyr]_2[SnCl_4]$ was performed by reacting [BMPyr]Cl and $SnCl_2$ with 2 : 1 ratio according to the following reaction: 2 [BMPyr]Cl + $SnCl_2$ → $[BMPyr]_2[SnCl_4]$.§ The reaction occurs already at room temperature when mixing the starting materials (Fig. 1(a)). The formation of $[BMPyr]_2[SnCl_4]$ is indicated by the occurring red-light emission and its increasing intensity. The product formation can be followed even with the naked eye (Fig. 1(b)). With intense mixing (see ESI‡), the synthesis is completed on a timescale of about 30 seconds. Whereas room-temperature mixing results in microcrystalline powder samples, crystallinity and emission intensity can be of course enhanced by certain heating. Thus, 45 °C for two weeks

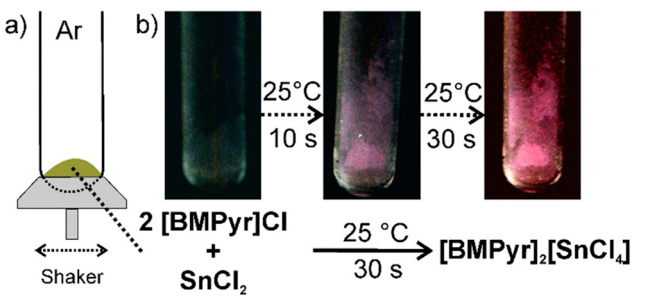

Fig. 1 Room-temperature synthesis of $[BMPyr]_2[SnCl_4]$: (a) scheme illustrating the mixing of [BMPyr]Cl and $SnCl_2$; (b) formation of $[BMPyr]_2[SnCl_4]$ indicated by increasing red emission on a timescale of 30 s of shaking (λ_{ex}: 366 nm).

Institut für Anorganische Chemie, Karlsruhe Institute of Technology (KIT), Engesserstrasse 15, 76131 Karlsruhe, Germany. E-mail: claus.feldmann@kit.edu

† Dedicated to Emma L. Wolf on the occasion of her birth.

‡ Electronic supplementary information (ESI) available: Analytical equipment, single crystal structure analysis and spectroscopic characterization. CCDC 2277913. For ESI and crystallographic data in CIF or other electronic format see DOI: https://doi.org/10.1039/d3cc03145d

or 80 °C for 6 hours result in macroscopic colourless and transparent single crystals with a size up to 1 mm^3.

According to single-crystal structure analysis, $[BMPyr]_2[SnCl_4]$ crystallizes with the monoclinic space group *C*2/*c* (ESI,‡ Table S1) and consists of $[BMPyr]^+$ cations and slightly distorted disphenoidal $[SnCl_4]^{2-}$ anions (Fig. 2(a)). The disphenoidal geometry is in accordance with the valence-shell-electron-pair-repulsion (VSEPR) model and reflects the presence of four Sn–Cl bonds and the lone-electron pair at Sn^{II+}, which together result in a distorted pseudo-trigonal-bipyramidal arrangement (Fig. 2(b)). Two shorter Sn–Cl distances of 246.4(1) pm (Sn–Cl2) are observed for the equatorial positions, whereas two longer distances of 281.9(1) pm (Sn–Cl1) occur for the axial positions. In principle, $[SnCl_4]^{2-}$ was observed before in compounds such as $[Co(NH_3)_6][SnCl_4][Cl]$.[6] In comparison to literature data (ESI,‡ Table S2), however, the $[SnCl_4]^{2-}$ anion in the title compound exhibits a higher symmetry with identical Sn–Cl distances on the equatorial and axial positions (Fig. 2(b)). $[Co(NH_3)_6][SnCl_4][Cl]$, for instance, shows different Sn–Cl distances for both positions (equatorial Sn–Cl with 246.7 and 252.6 pm; axial Sn–Cl with 266.9 and 300.3 pm).[6c] The Cl_{ax}–Sn–Cl_{ax} and Cl_{eq}–Sn–Cl_{eq} angles in the $[SnCl_4]^{2-}$ anion are 179.2(1)° and 93.8(1)°, which reflects the influence of the lone electron pair at Sn^{2+}. Like the Sn–Cl distances, these angles are different from literature data (*e.g.* $[Co(NH_3)_6][SnCl_4][Cl]$: Cl_{ax}–Sn–Cl_{ax}: 164.7°, Cl_{eq}–Sn–Cl_{eq}: 90°).[6] All distances in the $[BMPyr]^+$ cation are as expected and not discussed in detail (ESI,‡ Fig. S1).

Beside single crystal structure analysis, composition and purity of $[BMPyr]_2[SnCl_4]$ were validated by energy-dispersive X-ray spectroscopy (EDXS), Fourier-transform infrared (FT-IR) spectroscopy and differential thermal analysis and thermogravimetry (DTA-TG). EDXS shows the expected Sn : Cl ratio of 1 : 4. Most of the vibrations observed in FT-IR spectra can be related to the $[BMPyr]^+$ cation (Fig. 3(a) and ESI,‡ Fig. S2). Furthermore, a strong vibration at 500 cm^{-1} originates from ν(Sn–Cl).[7] Finally, the absence of any absorption at 3600–3000 cm^{-1} should be noticed and points to the absence of OH-related vibrations.

Thermally, $[BMPyr]_2[SnCl_4]$ turned out to be stable up to 200 °C (Fig. 3(b)). Thereafter, two-step decomposition occurs

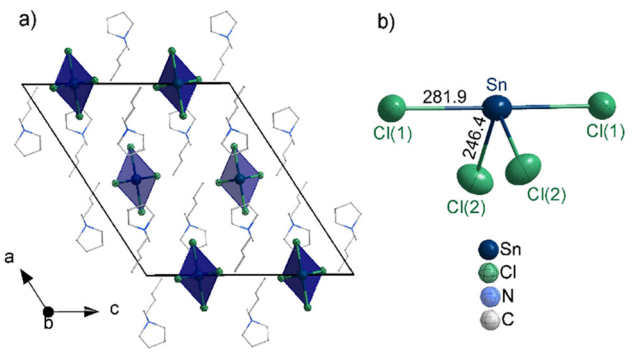

Fig. 2 Crystal structure of $[BMPyr]_2[SnCl_4]$: (a) unit cell ($[SnCl_4]^{2-}$ as blue polyhedron; $[BMPyr]^+$ as wires and sticks for clarity; see ESI,‡ Fig. S1 for details); (b) disphenoidal $[SnCl_4]^{2-}$ anion (distances in pm).

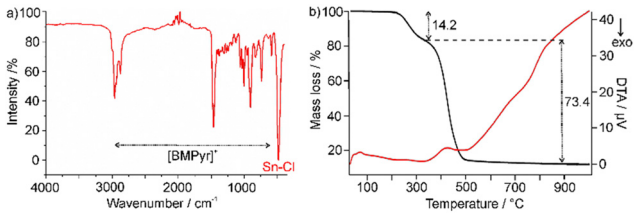

Fig. 3 Characterization of $[BMPyr]_2[SnCl_4]$: (a) FT-IR spectrum (see ESI,‡ Fig. S2 for comparison with [BMPyr]Cl); (b) DTA-TG analysis (heating rate: 5 K min^{-1}, atmosphere: Ar).

with a total mass loss of 87.6%, which can be related to the decomposition of the organic cation and the evaporation of $SnCl_4$ after disproportionation of Sn(II) to Sn(0) and Sn(IV) (calculated: 89.1%). Tin metal is observed as black solid remain with 12.4% (calculated: 10.9%). Interestingly, differential thermal analysis (DTA) does not show any endothermal peak indicating the melting point of the title compound below its thermal decomposition at 200 °C (Fig. 3(b)). Both starting materials have melting points ≥200 °C, too ([BMPyr]Cl: 198 °C; $SnCl_2$: 246 °C).[2,6a,8] Thus, starting materials and product can be excluded as potential liquid phases supporting a reaction at room temperature. In fact, $[BMPyr][SnCl_3]$ – formed as a first step of the Lewis acid–base reaction of [BMPyr]Cl and $SnCl_2$ – can be considered to be the compound with the lowest melting point (at about 80 °C).[6a,9] When taking a further reduction of the melting point for eutectic mixtures of $[BMPyr][SnCl_3]$ with the starting materials and/or the product into account, they can be expected to induce the room-temperature reaction and formation of $[BMPyr]_2[SnCl_4]$ just by mixing or at slightly elevated temperature. Finally, it must be noticed that $[BMPyr]_2[SnCl_4]$ – although being a solid – is a soft, sticky compound.

While the red emission of $[BMPyr]_2[SnCl_4]$ could be already used to visualize its formation (Fig. 1(b)), the optical properties were examined in more detail after optimized synthesis (80 °C, 6 h) with addition of minor amounts of $CaCl_2$ (2 mol%) as a flux. First of all, UV-Vis spectra were recorded, showing a steep absorption below 380 nm (Fig. 4(a)). Such steep absorption also points to the high crystallinity of the compound although prepared at low temperature.[10] By plotting the absorption coefficient $(F(R)h\nu)^2$ *versus* $(h\nu)$ in a Tauc plot, an indirect allowed optical band gap of 3.75 eV can be determined

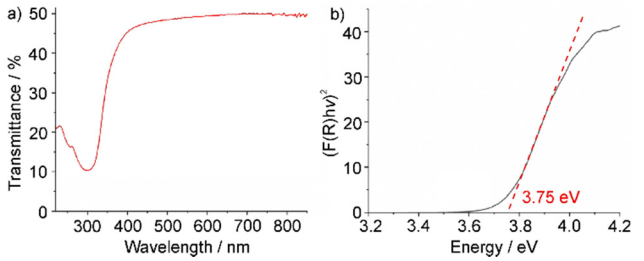

Fig. 4 Optical properties of $[BMPyr]_2[SnCl_4]$: (a) UV-Vis spectrum; (b) Tauc plot to determine the band bap.

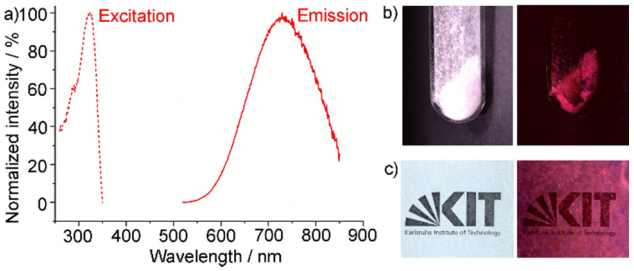

Fig. 5 Luminescence of $[BMPyr]_2[SnCl_4]$: (a) excitation (monitored at λ_{em}: 740 nm) and emission spectra (recorded at λ_{ex}: 320 nm); (b) photo of crystals in daylight and with UV-excitation (λ_{ex}: 366 nm); (c) thinfilm on glass plate in daylight and with UV-excitation (λ_{ex}: 366 nm).

(Fig. 4(b)), which is comparable to $SnCl_2$ as binary phase (3.8 eV).[11] Excitation spectra of $[BMPyr]_2[SnCl_4]$ also show strong absorption below 380 nm, which can be related to the valence-band to conduction-band transition (Fig. 5(a)). Emission spectra show intense deep-red emission at 600–850 nm with its maximum at 740 nm (Fig. 5(a)). This emission can be related to a $5s^1p^1 \rightarrow 5s^2p^0$ transition on Sn^{2+}.[12] The binary $SnCl_2$ also shows such Sn^{2+}-based emission (λ_{max}: 600 nm), but – in contrast to $[BMPyr]_2[SnCl_4]$ – together with conduction-band to valence-band emission (λ_{max}: 460 nm) of equal intensity.[11] Even more important, the emission of $SnCl_2$ is almost completely quenched at room temperature and becomes efficient only $\leq$60 K.[13]

Qualitatively, the red emission can be visualized after excitation with a mercury discharge lamp (λ_{ex}: 366 nm) or a UV-LED (λ_{ex}: 280–350 nm) (Fig. 5(b)). The photoluminescence process was quantified by determining the absolute quantum yield following the method given by Friend *et al.*[14] Accordingly, a surprisingly high quantum yield of 25–30% was already obtained after room-temperature synthesis and simple mixing of the starting materials (Fig. 1). With an optimised synthesis (80 °C, 6 h, addition of 2% of $CaCl_2$ as a flux), a remarkable quantum yield of 88 ± 3% was obtained. This value belongs to the highest quantum yields reported for Sn^{2+}-based emission.[15]

In principle Sn^{2+}-based emission is well-known and can be very efficient as a parity-allowed s–p transition.[12,15b] Examples, first of all, include conventional lamp phosphors such as $Ba_2Li_2Si_2O_7:Sn^{2+}$, $Ca_3(PO_4)_2:Sn^{2+}$ or $Ca_5(PO_4)_3F:Sn^{2+}$ (Table 1).[15b,16] In difference to $[BMPyr]_2[SnCl_4]$, herein, Sn^{2+} is present only as a dopant (1–5 mol%) to avoid concentration quenching.[12,15b] Moreover, metal oxides with high lattice energy are applied and prepared at high temperature ($\geq$500 °C) to guarantee high crystallinity and low defect concentration and, in sum, to realize a high quantum yield.[15b,16] In addition to conventional phosphors, organo-tin halides came up with the discovery of methylammonium lead iodide and also can show luminescence.[15a] In particular, this holds for organo-tin halides with the heavier halogens bromine and iodine (Table 1). Due to their small bandgap, these compounds show semiconductor-type conduction-band to valence-band emission instead of Sn^{2+}-based s–p transition (Table 1).[15a,17] High quantum yields (>80%) of such semiconductor-type luminescence are specifically observed for spatially restricted systems, such as quantum dots (0 D)[18] or nanolayers (2 D)[19] (Table 1).

In difference to bromides and iodides, the quantum yield of organo-tin chlorides is low ($\leq$20%).[20] Taken together, a quantum yield $\geq$50% for s–p-based emission as observed for $[BMPyr]_2[SnCl_4]$ with molar amounts of Sn^{2+} tin is unusual. The high quantum yield is even more surprising taking the low temperature of synthesis and the limited lattice energy into account. The promising luminescence of $[BMPyr]_2[SnCl_4]$ can be attributed to the good crystallization even at low temperature and the low sensitivity to lattice defects. Furthermore, the large-sized cation leads to a large distance between the luminescent Sn^{2+} centres (shortest $Sn^{2+}\cdots Sn^{2+}$ distance: 890.2(2) pm), so that concentration quenching is avoided despite of molar quantities of Sn^{2+}.

Similar to organo-metal halides like $[CH_3NH_3]PbI_3$,[4] $[BMPyr]_2[SnCl_4]$ is also soluble in DMSO or DMF, which offers the option for solvent-based processing. As a proof-of-the-concept, here, a solution of the title compound in DMSO was deposited on a glass plate (Fig. 5(c)). After slow evaporation of

Table 1 Luminescence properties of $[BMPyr]_2[SnCl_4]$ in comparison to literature data on Sn^{2+}-containing compounds

Compound	Maximum of excitation/nm	Maximum of emission/nm	Quantum yield/%
$[BMPyr]_2[SnCl_4]$ (title compound)	322	740	88 ± 3%
$Ba_2Li_2Si_2O_7:Sn^{2+}$ (5 mol%)[15b]	254	429	60–70
$Ca_3(PO_4)_2:Sn^{2+}$ (5 mol%)[16a]	254	646	80–90
$Ca_5(PO_4)_3F:Sn^{2+}$ (10 mol%)[16b]	254	413	80–90
$CsSnCl_3$[20a]	420	490	<1
$[C_6N_2H_{16}Cl]_2[SnCl_6]$[20b]	365	450	8
Cs_4SnBr_6[20c]	365	534	21
$[C_6H_{13}NH_3]_2[SnBr_4]$[17a]	335	618	35
$[C_8H_{17}NH_3]_2[SnBr_4]$[17a]	344	610	82
$[C_{12}H_{25}NH_3]_2[SnBr_4]$[17a]	338	603	60
$[C_{18}H_{35}NH_3]_2[SnBr_4]$[17a]	339	623	52
0D-$[(PEA)_4SnBr_6][(PEA)Br] \times (CCl_2H_2)_2$[18]	304	566	90
2D-$[(PEA)_4SnBr_6][(PEA)Br] \times (CCl_2H_2)_2$[18]	304	566	<1
$[Bmpip]_2[SnBr_4]$[17b]	405	665	75
2D-$[C_8H_{17}NH_3]_2[SnI_4]$[19]	340	670	95

PEA: phenylethylammonium; Bmpip: 1-buthyl-1-methyl-piperidinium

DMSO at room temperature, a transparent thinfilm of $[BMPyr]_2[SnCl_4]$ was obtained, which also shows intense red emission (Fig. 5(c)). Based on its simple synthesis, intense emission, high quantum yield and optional solvent processing, $[BMPyr]_2[SnCl_4]$ could become interesting as a luminescent material for deep-red or infrared emitting LEDs.[21]

In conclusion, $[BMPyr]_2[SnCl_4]$ is obtained as a novel organo-tin(II) halide. The compound can be prepared just by mixing of the starting materials [BMPyr]Cl and $SnCl_2$ at room temperature, which can be followed by the increasing deep-red Sn^{2+}-based emission (λ_{max}: 740 nm). Even after mixing at room temperature, a quantum yield of 25–30% was achieved. With optimised synthesis conditions (*i.e.*, 80 °C, 6 h, addition of 2% of $CaCl_2$ as a flux), a quantum yield of 88 ± 3% was obtained, which is extraordinarily high for Sn^{2+}-based emission, in general. The reaction proceeds with quantitative yield and without addition of solvents. It is promoted by $[BMPyr][SnCl_3]$ (forming an eutectic with starting materials and/or product) as intermediately formed ionic liquid, whereas the starting materials as well as the product exhibit melting points ≥200 °C. In addition to the unusual synthesis near room temperature (≤100 °C) *via* a simple reaction with quantitative yield, the deep-red emission (600–850 nm) and the high quantum yield (88 ± 3%) as well as optional solvent processing potentially can make $[BMPyr]_2[SnCl_4]$ interesting as a luminescent material for deep-red or infrared emitting thinfilms and LEDs.

The authors thank the Deutsche Forschungsgemeinschaft (DFG) for funding within the project ''Crown ether coordination compounds with unusual structural and optical properties (Crown I)''.

Conflicts of interest

The authors declare no conflicts of interest.

Notes and references

§ Experimental: all reactions and sample handling were carried out under dried argon atmosphere using standard Schlenk techniques or glove boxes (MBraun Unilab, $c(O_2, H_2O) < 0.1$ ppm). Reactions were performed in Schlenk flasks and glass ampoules that were evacuated ($p < 10^{-3}$ mbar), heated and flashed with argon three times prior to use. The starting materials $SnCl_2$ (99.99%, ABCR) and $CaCl_2$ (99.99%, ABCR) were used as received, whereas [BMPyr]Cl (99%, Iolitec) was dried under reduced pressure (10^{-3} mbar) at 130 °C for 48 h.

$[BMPyr]_2[SnCl_4]$: 187.4 mg (2 eq, 1.055 mmol) of [BMPyr]Cl and 100 mg (1 eq, 0.527 mmol) $SnCl_2$ were treated in three different ways. The starting materials can be intensely mixed for 30 seconds (VWR Digital Vortex Mixer, see ESI‡ for details) in a sealed glass ampoule under argon at room temperature. The starting materials can be also heated for 2 weeks at 40 °C in a sealed glass ampoule under argon. Finally, in an optimized synthesis for optimal luminescence properties, 1.2 mg of $CaCl_2$ (0.02 eq, 0.011 mmol) were added as a flux to the starting materials, which were then heated for 6 hours at 80 °C in a sealed glass ampoule under argon. After mixing or after slow cooling to room temperature (1 K h^{-1}), $[BMPyr]_2[SnCl_4]$ was obtained as colorless, needle-shaped crystals with quantitative yield. The title compound is sensitive to moisture and needs to be stored in dry air or under nitrogen or argon.

Crystal structure analysis: Further details regarding the crystal structure investigation may be obtained from the Fachinformationszentrum Karlsruhe, D-76344 Eggenstein-Leopoldshafen (Germany) on quoting the depository number CCDC 2277913.†

1 *Modern Inorganic Synthetic Chemistry*, ed. R. Xu and Y. Xu, Elsevier, Amsterdam, 2nd edn, 2017.
2 N. N. Greenwood and A. Earnshaw, *Chemistry of the Elements*, Butterworth-Heinemann, Oxford, 2nd edn, 1998.
3 (*a*) T. Zhang, T. Doert, H. Wang, S. Zhang and M. Ruck, *Angew. Chem., Int. Ed.*, 2021, **60**, 22148–22165; (*b*) D. Freudenmann, S. Wolf, M. Wolff and C. Feldmann, *Angew. Chem., Int. Ed.*, 2011, **50**, 11050–11060.
4 L. Ke, S. Luo, X. Ren and Y. Yuan, *J. Phys. D*, 2021, **54**, 163001.
5 M. A. Green, A. Ho-Baillie and H. J. Snaith, *Nat. Photonics*, 2014, **8**, 506–514.
6 (*a*) M. Currie, J. Estager, P. Licence, S. Men, P. Nockemann, K. R. Seddon, M. Swadzba-Kwasny and C. Terrade, *Inorg. Chem.*, 2013, **52**, 1710–1721; (*b*) C. Zhong, T. Sasaki, A. Jimbo-Kobayashi, E. Fujiwara, A. Kobayashi, M. Tada and Y. Iwasawa, *Bull. Chem. Soc. Jpn.*, 2007, **80**, 2365–2374; (*c*) H. J. Haupt, F. Huber and H. Preut, *Z. Allg. Anorg. Chem.*, 1976, **2**, 97–103.
7 (*a*) I. Wharf and D. F. Shriver, *Inorg. Chem.*, 1969, **8**, 914–925; (*b*) M. Liebertseder, S. Wolf and C. Feldmann, *Z. Anorg. Allg. Chem.*, 2021, **647**, 2147–2156.
8 U. Domanska, M. Wieckowski and P. Okuniewska, *Fluid Phase Equilib.*, 2017, **447**, 84–94.
9 S. Wolf, S. Seidel, J. Treptow, R. Köppe, P. Roesky and C. Feldmann, *Inorg. Chem.*, 2022, **61**, 4018–4023.
10 J. Wong, S. T. Omelchenko and H. A. Atwater, *ACS Energy Lett.*, 2021, **6**, 52–57.
11 J.-I. Nara and S. Adachi, *J. Appl. Phys.*, 2011, **109**, 083539.
12 J. Nara and S. Adachia, *J. Appl. Phys.*, 2011, **109**, 083539.
13 G. Blasse and B. C. Grabmaier, *Luminescent Materials*, Springer, Berlin, 1994.
14 J. C. de Mello, H. F. Wittmann and R. H. Friend, *Adv. Mater.*, 1997, **9**, 230.
15 (*a*) X. Li, X. Gao, X. Zhang, X. Shen, M. Lu, J. Wu, Z. Shi, V. L. Colvin, J. Hu, X. Bai, W. W. Yu and Y. Zhang, *Adv. Sci.*, 2021, **8**, 2003334; (*b*) W. M. Yen, S. Shionoya and H. Yamamoto, *Phosphor Handbook*, CRC Press, Boca Raton, 2006.
16 (*a*) E. R. Kreidler, *J. Electrochem. Soc.*, 1971, **118**, 923–929; (*b*) H. J. Jenkins, A. H. McKeag and P. W. Ranby, *J. Electrochem. Soc.*, 1949, **96**, 1–12.
17 (*a*) Y. Liu, A. Wang, J. Wu, C. Wang, Z. Li, G. Hu, S. Sui, J.-X. She, W. Meng, W. Li and Z. Deng, *Mater. Adv.*, 2021, **2**, 1320–1327; (*b*) V. Morad, Y. Shynkarenko, S. Yakunin, A. Brumberg, R. D. Schaller and M. V. Kovalenko, *J. Am. Chem. Soc.*, 2019, **141**, 9764–9768.
18 L.-J. Xu, H. Lin, S. Lee, C. Zhou, M. Worku, M. Chaaban, Q. He, A. Plaviak, X. Lin, B. Chen, M.-H. Du and B. Ma, *Chem. Mater.*, 2020, **32**, 4692–4698.
19 A. Wang, Y. Guo, Z. Zhou, X. Niu, Y. Wang, F. Muhammad, H. Li, T. Zhang, J. Wang, S. Nie and Z. Deng, *Chem. Sci.*, 2019, **10**, 4573–4579.
20 (*a*) T. C. Jellicoe, J. M. Richter, H. F. J. Glass, M. Tabachnyk, R. Brady, S. E. Dutton, A. Rao, R. H. Friend, D. Credgington, N. C. Greenham and M. L. Böhm, *J. Am. Chem. Soc.*, 2016, **138**, 2941–2944; (*b*) G. Song, M. Li, Y. Yang, F. Liang, Q. Huang, X. Liu, P. Gong, Z. Xia and Z. Lin, *J. Phys. Chem. Lett.*, 2020, **11**, 1808–1813; (*c*) L. Tan, W. Wang, Q. Li, Z. Luo, C. Zou, M. Tang, Z. Min, L. Zhang, J. He and Z. Quan, *Chem. Commun.*, 2020, **56**, 387–390.
21 M.-H. Fang, Z. Bao, W.-T. Huang and R.-S. Liu, *Chem. Rev.*, 2022, **122**, 11474–11513.

